

MAAS: Multi-modal Assignment for Active Speaker Detection

Juan León Alcázar¹, Fabian Caba Heilbron², Ali Thabet¹, and Bernard Ghanem¹

¹King Abdullah University of Science and Technology, ²Adobe Research,

¹{alcazahj, ali.thabet, bernard.ghanem}@kaust.edu.sa; ²caba@adobe.com;

Abstract

Active speaker detection requires a solid integration of multi-modal cues. While individual modalities can approximate a solution, accurate predictions can only be achieved by explicitly fusing the audio and visual features and modeling their temporal progression. Despite its inherent multi-modal nature, current methods still focus on modeling and fusing short-term audiovisual features for individual speakers, often at frame level. In this paper we present a novel approach to active speaker detection that directly addresses the multi-modal nature of the problem, and provides a straightforward strategy where independent visual features from potential speakers in the scene are assigned to a previously detected speech event. Our experiments show that, an small graph data structure built from a single frame, allows to approximate an instantaneous audio-visual assignment problem. Moreover, the temporal extension of this initial graph achieves a new state-of-the-art on the AVA-ActiveSpeaker dataset with a mAP of 88.8%.

1. Introduction

Active speaker detection aims to identify the current speaker (if any) from a set of candidate face detections from an arbitrary video. This research problem is an inherently multi-modal task that requires the integration of subtle facial motion patterns and the characteristic waveform of speech. Despite its multiple applications such as speaker diarization [3, 43, 45, 47], human-computer interaction [15, 57] and bio-metrics [33, 39], the detection of active speakers in-the-wild remains an open problem. Recently, the AVA Active-Speaker dataset and benchmark [40] has provided the first large-scale standard benchmark for evaluating this problem, thereby enabling it to be approached with modern machine learning techniques.

Current approaches for active speaker detection are based on recurrent neural networks [2, 40, 42], or 3D convolutional models [1, 6, 59]. Their main focus is to jointly model audio and visual streams to maximize the single speaker prediction confidence over short sequences. While

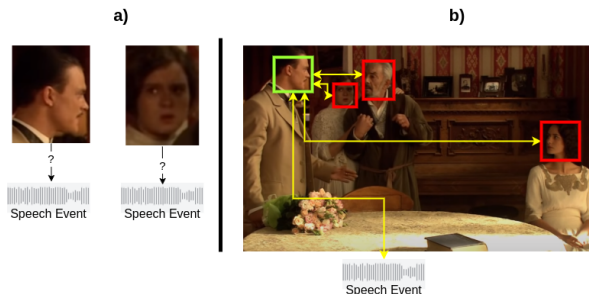


Figure 1. **Feature assignment for active speaker detection.** The active speaker detection task is highly ambiguous, even if we analyze joint audiovisual information, unrelated facial gestures can easily resemble the natural motion of the lips while speaking. In **a)** we show two face crops from a sequence where a speech event was detected, the gestures, illumination and capture angle make it hard to assess which one (if any) is the active speaker. Our strategy **b)** focuses on the attribution of speech segments in video. If a speech event is detected, we holistically analyse every other speaker along with the audio track to discover the most likely active speaker.

these approaches are effective in single speaker scenarios, they are overly simplified for the general multi-speaker case. In such multi-speaker setting, a single speech segment must be matched to multiple candidate speakers and attributed to only one of them.

The general multi-speaker scenario has two major challenges. First, the presence of multiple speakers allows for incorrect facial-voice assignments. For instance, false positives emerge when facial gestures closely resemble the motion patterns observed while speaking (e.g. laughing, grinning). Second, it must enforce temporal consistency over multi-modal data, which quickly evolves over time, e.g., when active speakers switch during a fluid conversation. Consequently, an accurate method for active speaker detection requires a joint analysis over every speaker’s facial gestures and the audio of the scene, assigning the audio features to its most likely source visual features. Figure 1 illustrates some of the challenges in active speaker detection, and a general insight of our approach.

In this paper, we address the general multi-speaker problem in a principled manner. Our key insight is that instead of optimizing active speaker predictions over individual audiovisual embeddings, we can jointly model a set of visual representations from every speaker in the scene, along with a single audio representation estimated from the shared audio track. While simple, this modification allows us to map the active speaker detection task into an assignment problem, whose goal is to match multiple visual representations with a singleton audio embedding.

Our approach the “multi-modal assignment for active speaker detection” (MAAS) relies on multi-modal graph neural networks [26, 49] to approach the local (frame-wise) assignment problem, but is flexible enough to also propagate information from a long-term analysis window by directly updating the underlying graph connectivity. In this framework, we define the active speaker as the local visual representation with the highest affinity to the audio embedding. Our empirical findings highlight that reformulating the problem into a multi-modal assignment problem, brings relevant improvements over current state-of-the-art methods. On the Ava Active speaker benchmark, MAAS outperforms every other method by at least 1.7%, additionally, when we compare our single frame approach with state-of-the-art methods that also analyze a single frame, MAAS brings a performance boost of at least 1.1%.

Contributions. This paper proposes a novel strategy for active speaker detection, that learns multi-modal relationships between audio tracks and facial features by directly sharing information across domains. Our work brings two contributions:

- (1) We provide a novel formulation for the active speaker detection problem. It explicitly matches the speaker’s visual features to a shared audio embedding of the scene (Section 3.2).
- (2) We empirically show that this assignment problem can be solved by leveraging Graph Convolutional Networks (GCNs), achieving flexibility on the graph structure, and obtaining state of the art results (Section 4.1).

To ensure reproducible results and promote future research, all the resources of this project, including source code, model weights, and official benchmark results, will be publicly available.

2. Related Work

Active Speaker Detection. In the realm of multi-modal learning, different information sources are fused with the goal of establishing a more effective representation than could be obtained from each source individually [35]. In the video domain, a common multi-modal paradigm involves combining representations from both

visual and audio features [4, 7, 21, 32, 33, 36, 48]. Such representations have attracted the interest of the com-

puter vision community, as they allow exploring new approaches to well established problems, such as person re-identification [32, 24, 54], audio-visual synchronization [1, 8, 9], speaker diarization [43, 47, 58], bio-metrics [33, 39], and audio-visual source separation [4, 21, 36, 40, 48]. Active speaker detection is a special instance of audiovisual source separation, where sources are the visible persons in a video, and the goal is to detect and assign a segment of speech to one of those candidates. The selected candidate is known as the active speaker [40].

The work of Cutler *et al.* [11] pioneered research in active speakers detection in the early 2000s. Their proposal detected correlated audiovisual signals by means of a time-delayed neural network [46]. Some follow up works [13, 41] approached the task relying only on visual information, focusing strictly on the evolution of facial gestures. Such visual-only modeling was possible as they addressed a simplified version of the problem with a single candidate for the speech attribution. Recent works [5, 9] have approached the more general multi-speaker scenario and relied on fusing multi-modal information from individual speakers.

A parallel corpus of work has focused on audiovisual feature alignment, which resulted in methods that rely on audio as the primary source of supervision [4], or as an alternative to jointly train a deep audiovisual embedding [7, 9, 34, 44]. While these approaches enabled more accurate active speaker detection, they are still limited by the lack of a large-scale testbed for training and benchmark, preventing the use of modern machine learning techniques and the application to in-the-wild active speaker detection.

To address the lack of a large scale testbed, the work of Roth *et al.* [40], introduced the AVA-ActiveSpeaker dataset and benchmark, the first large-scale video dataset for the active speaker detection task. Upon the release of this dataset and its baseline, some novel approaches have been published. In the AVA-ActiveSpeaker challenge of 2019, Chung *et al.* [6] presented and improved architecture of their previous work [9], which trained a large 3D model that relies on large-scale audiovisual pre-training [34]. Zhang *et al.* [59] also leveraged a hybrid 3D-2D architecture with large-scale pre-training [9, 10]. This method achieved its best performance when the feature embedding was optimized using contrastive loss [17]. Follow up works focused on modeling an attention process over face tracks, where attention was estimated either from the audio alignment [1], or from an ensemble of speaker features [2].

Current approaches to active speaker detection focus on estimating an audiovisual feature embedding from a single frame or a short clip. We depart from these ideas and approach the multi-modal scenario in a novel way by establishing explicit relationships between a set of independent visual features and a single audio feature. As consequence we do not focus on estimating a feature embedding that en-

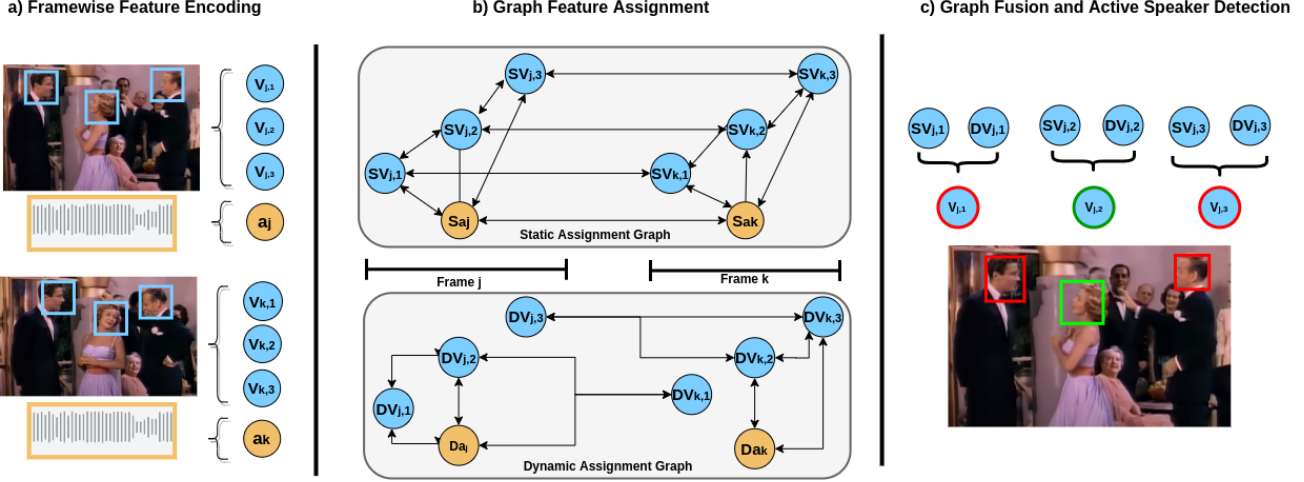


Figure 2. **Overview of MAAS Pipeline.** **a)** Our approach begins by sampling independent audio and video features. Video features (cyan) are extracted from a stack of face crops that belong to single person. Audio features (yellow) are estimated from the audio-spectrogram and are shared at the frame level. **b)** We model two feature graphs one with static connections that model local temporal relation between the audio track, the visible person, and their temporal relations; in parallel, we also allow a secondary stream in the network to discover relationships given the estimated feature embeddings. **c)** Finally, we optimize the network so that a subset of nodes approximates the temporal support of speech events, while the remainder optimize the affinity of visual features to the current audio. We select the active speaker (green bounding box) as the most likely speaker to have generated the audio.

ables binary classification, *i.e.* active speaker vs. silent. Instead, we focus on dynamically modeling affinities between the involved modalities following one rule: if speech patterns are detected they must be assigned to one of the independent speakers on the screen.

Graph Convolutional Networks (GCNs). GCNs [26] have recently gained popularity, due to the greater interest in non-Euclidean data. In computer vision, GCNs have been successfully applied to scene graph generation [22, 31, 38, 52, 56], 3D understanding [16, 29, 49, 51], and action recognition in video [20, 53, 55]. In MAAS we design a DeepGCN-like architecture [27, 28, 30], that addresses a special scenario, namely the multi-modal nature of audiovisual data. We rely on the well known EdgeConv operator [49], to model interactions between different modalities on graph nodes identified across multiple frames. This enables us to model both the multi-modal relations and the temporal dependencies in a single graph structure.

3. Multi-modal Active Speaker Assignment

Our approach to the active speaker problem is based on a simple yet effective idea: Instead of assessing the likelihood of individual audiovisual patterns to belong to an active speaker, we directly model the correspondence between the local audio patterns and the visual appearance of all the individuals present in the scene. This approach is motivated by the nature of the active speaker problem, which first identifies if any speech patterns are present, and

then attributes those patterns to a single speaker¹.

Overall, our approach simultaneously solves three sub-tasks: First, we detect speech events in a short-term temporal window. Second, we iterate over all the visible speakers in a single frame, and decide which one is most likely to be an active speaker given the local information. Third, we extend this frame-level analysis along the temporal dimension, leveraging the inherent temporal consistency of video data to improve frame level predictions. Figure 2 contains an overview of our approach.

3.1. Frame Level Video Features

Following recent works [2, 40, 59], we extract the initial frame level features from a two-stream convolutional encoder. The visual stream takes as input a tensor of dimensions $H \times W \times (3c)$, where H and W are the images width and height, and c is the number of time consecutive face crops obtained from a single tracklet. Similar to [40], we transform the original audio waveform into a Mel-spectrogram, and use it as input for the audio stream.

Our approach requires independent audio and video features which are later fused in the assignment process. To obtain these independent features (and to make fair comparison to state-of-the-art techniques), we train a joint model as described by [2], but at inference time we drop the final two layers where the feature fusion and final prediction are performed. This results in independent feature embeddings for

¹We can assume that a single speaker must be attributed, as simultaneous active speakers and out of screen speakers are very rare.

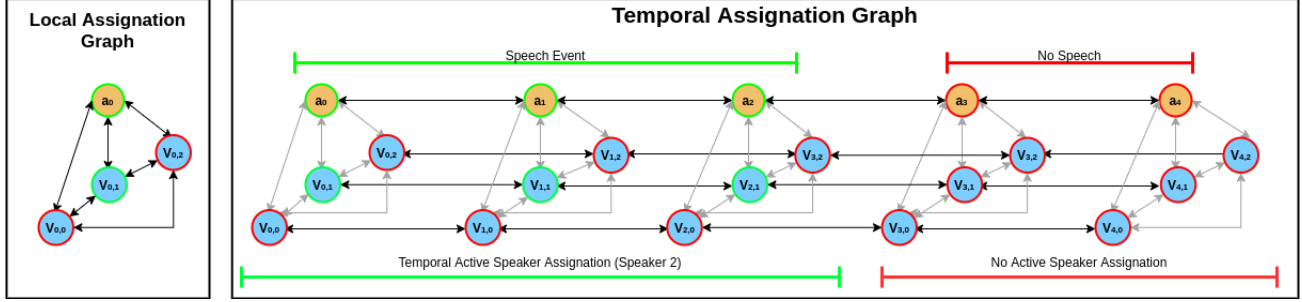


Figure 3. **Assignment Graphs.** The base static graphs for MAAS are composed of multi-modal nodes, visual nodes (Cyan), and audio nodes (Yellow). The local Assignment Graph (left) defines frame level connectivity of the individual features. The Temporal Assignment Graph (right) is composed of multiple local graphs (5 in the figure) and defines a temporal extension of the frame-level relations (we depict local relations in light gray to avoid visual clutter). While local graphs solves an instantaneous assignment problem. The temporal graph optimizes a subset of nodes thereby incorporating temporal information in the individual local graphs.

the audio and video stream. A forward pass at time t of a frame with N possible speakers (visible persons), will yield $N + 1$ feature vectors, one for the shared audio (\mathbf{a}_t) and N independent visual descriptors $\mathbf{v}_t = \{v_{t,0}, v_{t,1}, \dots, v_{t,n-1}\}$ extracted from the N visible persons in the screen (see Figure 2a)).

We define the set of features at time t as the shared audio feature and the individual visual features of all visible persons $\mathbf{s}_t = \{\mathbf{a}_t \cup \mathbf{v}_t\}$. The feature set \mathbf{s}_t is used for the optimization of the basic graph structure of our proposal, the Local Assignment Network.

3.2. Local Assignment Network

We model the local assignment problem by generating a directed graph, based on features \mathbf{s}_t . Our local graph consists of an audio node and one video node for each potential speaker. We create bidirectional connectivity between the audio node and each visual node, as well as bidirectional connectivity between all visual nodes. Thus leveraging a GCN that operates on a small graph generated from \mathbf{s}_t .

Figure 3 (left) illustrates this graph structure. We name this graph structure the Local Assignment Graph, and the GCN that operates over it as Local Assignment Network (LAN).

LAN’s goals are two-fold: (i) to detect local speech events, and (ii) if there is a speech event, to assign the most likely active speaker from the set of candidates. We achieve these two goals by fully supervising every node in LAN. Visual nodes are

supervised by the individual ground-truth, l_{vt} , of the corresponding speaker, while audio ones get a binary ground-truth label indicating whether there is at least one active speaker, that is: $\max(\{l_{0,t}, l_{1,t}, \dots, l_{n,t}\})$. The LAN will discover active speakers at frame-level whenever the audio node and at least one of the video nodes have positive predictions.

3.3. Temporal Assignment Networks

While then LAN is effective at finding local correspondences between audio patterns and visible faces, it models information sampled from short video clips (\mathbf{s}_t). Such sampling strategy can lead to inaccurate predictions from noisy or ambiguous local estimations (e.g. audio noise, small faces, blur, etc.). We approach this limitation by extending our temporal analysis and include additional information from adjacent frames.

We extend the local assignment graph by sampling the feature set \mathbf{s}_t over a longer temporal window $w = [i, i + 1, \dots, t, \dots, j]$. Over this sampling window, we define $\mathbf{s}_w = [\mathbf{s}_i, \mathbf{s}_{i+1}, \dots, \mathbf{s}_t, \dots, \mathbf{s}_j]$, this results in $j - i$ independent local graph structures (one for every time step). We augment this set of independent graphs, by adding temporal links between time adjacent representations of frame-level features. We follow two rules to build these connections: we create temporal connections between time adjacent audio nodes, and we create temporal connections between time adjacent video nodes only if they belong to the same person. No additional cross-modal connections are built. We name the resulting graph the Temporal Assignment Graph, which allows for information flow between time adjacent audio and video features, thereby achieving temporal consistency in the audio and video modalities. In Figure 3 (right) we present an outline on this graph structure.

We build a GCN over the extended graph topology, which we call it the Temporal Assignment Network (TAN). TAN allows us to directly identify speech segments as continuous positive predictions over audio nodes. Likewise, it detects active speech segments over continuous predictions for same-speaker video features.

3.4. Dynamic Stream & Global Prediction

Finally, we account for potential connection patterns that go beyond our initial insights. To do so, we augment our

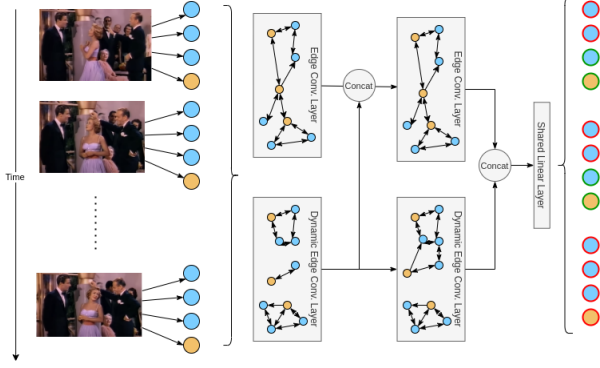


Figure 4. **Graph Neural Network Architecture.** Our graph neural network implements a two stream architecture. The first stream (top) uses the dynamic edge convolution operator and works over LAG or TAG graphs. The second stream (bottom) relies on dynamic edge convolutions and complements the feature embedding discovered by the static stream by means of slow fusion. After every layer we fuse the feature from the dynamic and static stream and use them as input for the next layer.

method and define a second stream that will work on the very same data as the static stream (including multiple temporal timestamps), but we do not specify a graph structure. Instead, we aim at creating dynamic graphs structures based on the node distribution on the feature space. In this stream, we allow the neural network to estimate an arbitrary graph by calculating the K nearest neighbors and establish edges between the neighbouring nodes [50].

The final prediction is achieved by slow fusion [23, 53]. At every layer, we merge the feature set from the dynamic layer with the feature set from the static layers. The final prediction is achieved using a shared fully connected layer over every node.

3.5. Training and Implementation Details

Following [2, 40], we implement a two-stream feature encoder based on the Resnet-18 architecture [18] initialized with ImageNet [12] weights. We perform the same modifications at the first layer to adapt for the modified input tensors (stack of face crops, and spectrogram). We train this neural network end-to-end using the Pytorch library [37] for 100 epochs with the ADAM optimizer [25]. We use 3×10^{-4} as initial learning rate which decreases with annealing of $\gamma = 0.1$ at epochs 40 and 80. We augment the input videos via random flips and corner crops. Note that we do not implement any large scale pre-training beyond ImageNet. We also incorporate the sampling strategy proposed by [2] as we also observe large overfitting when sampling over the full image dataset.

At training time we follow the supervision strategy suggested by [40], where two extra auxiliary loss functions $\mathcal{L}_a, \mathcal{L}_v$ are adapted on the final layer of the audio and

video stream, this favors the estimation of useful features from both streams, a critical feature for our approach as we extract independent audio and video features from each stream.

Training MAAS We implement MAAS (along with the LAN and TAN networks) using the PyTorch Geometric library [14]. We choose edge-convolution [50] to propagate the neighboring information between nodes. Our design includes a network model with 4 edge convolutional layers, each with filters of 64 dimensions. Before the first edge convolutional layer, we apply dimensionality reduction to map features from their original 512 dimension to 64, we empirically find that this dimensionality reduction favors the final performance and largely reduces the computational resources required by the network. As we handle data from different modalities, we use two different independent connected layers for dimensionality reduction, one exclusively for video features, one solely for audio features.

Dynamic Stream As outlined in section 3.3, the final version of our network is a two stream model. Both streams use the same input data, and their architecture is identical; however, one works over a static graph, and the other uses a dynamic connectivity pattern. In practice, we replicate the static stream and drop the definition of the static graph, and use the dynamic version of the edge-convolution [49], allowing for a dynamic graph estimation at every layer.

We train two networks MAAS-LAN and MAAS-TAN using the same procedure and set of hyper-parameters, the only difference being the underlying graph structure. We use the Pytorch library and the ADAM optimizer with an initial learning rate of 1×10^{-4} and train for 4 epochs. We use random initialization, and implement a pre-activation [19] linear layer (Batch Normalization \rightarrow ReLu Activation \rightarrow Linear Layer) as the operation to map the concatenated node features inside the edge convolution.

4. Experimental Validation

In this section, we provide an empirically analysis of our proposed method. We focus on the large-scale AVA-ActiveSpeaker dataset [40] to asses the performance of our method. This section is divided in three parts. First, we compare our approach with state-of-the-art techniques. Then, we ablate our proposal and analyse all of our individual design choices. Finally, we test our method on known challenging scenarios to explore common failure modes.

AVA-ActiveSpeaker Dataset. The AVA-ActiveSpeaker dataset [40] is the first large-scale testbed for the active speaker detection problem. It is composed of 262 Hollywood movies: 120 of those on the training set, 33 on

Method	mAP
<i>Validation Set</i>	
MAAS-TAN (Ours)	88.8
Alcazar <i>et al.</i> [2]	87.1
Chung <i>et al.</i> (Temporal Convolutions) [6]	85.5
Alcazar <i>et al.</i> (Temporal Context) [2]	85.1
Chung <i>et al.</i> (LSTM) [6]	85.1
MAAS-LAN (Ours)	85.1
Zhang <i>et al.</i> [59]	84.0
Sharma <i>et al.</i> [42]	82.0
Roth <i>et al.</i> [40]	79.2

Table 1. **Comparison with State-of-the-art methods.** We compare the performance of our proposal, and report the performance of state-of-the-art methods in the AVA Active Speakers validation set. Results are calculated with the official evaluation tool as published by [40]. We report an improvement over state-of-the-art methods of 1.7% MAP.

validation, and the remaining 109 on testing. The AVA-ActiveSpeaker dataset contains normalized bounding boxes for 5.3 million faces: 2.6M training, 0.76M validation, and 2.0M testing, all manually curated from automatic detections. These face bounding boxes are obtained over 15-minute non-overlapping segments. Facial detections occur at an average rate of 22fps and are manually linked across time to produce face tracks (tracklets) depicting a single identity (actor). In the AVA-ActiveSpeaker dataset, each face detection is labeled as speaking, speaking but not audible, or non-speaking. At inference time, the goal is to estimate a confidence score for a speaking face.

All the results reported in this paper correspond to those estimated with the official evaluation tool provided by the dataset creators, which computes the mean average precision (mAP) metric.

4.1. Comparison with the State-of-the-art

We begin our result analysis by comparing our proposal to state-of-the-art methods. The results reported for MAAS-TAN are obtained from a two stream model composed of 13 temporally linked local graphs. At training time, We set $K = 3$ for the number of nearest neighbors in the dynamic stream, and limit the number of video nodes to 4 per frame. The results reported for the MAAS-LAN are obtained from a two stream model which includes a single timestamp and 4 video nodes. For sequences with 5 or more visible speakers, we make sure that one video node contains the features from the active speaker, and randomly sample the remaining 3. If no active speaker is present, we just randomly sample 4 speakers without replacement. At inference time, we split the speakers in non overlapping groups of 4, and forward multiple times. Results in the validation set are summarized in Table 1.

Our best model outperforms every other method reported

in the AVA-ActiveSpeaker validation set. We highlight two aspects of these results: First, at 88.8% mAP our MAAS-TAN network outperforms the best results reported on this dataset by at least 1.7%. It must be noted that some state-of-the-art methods [6, 59] rely on large 3D models and large scale audiovisual pre-training, while MAAS uses only the standard ImageNet initialization for both streams. Second, while the MAAS-LAN network does not achieve state-of-the-art performance, it outperforms every other method that does not rely on long-term temporal evaluations [40, 59]. It also remains competitive to those methods that rely only on long-term context [6, 2], being outperformed only by the temporal version of [2] by a margin of 0.6%, and falling 2.1% behind the full method of [2] (temporal context and multi-speaker).

4.2. Ablation Analysis

After assessing the performance of our proposal against state-of-the-art techniques, we ablate our best method (MAAS-TAN) to validate the individual contributions of every design choice, namely: network depth, network width, independent stream contributions and the number of neighbors for the dynamic stream.

Network Architecture We begin the assessment of our design decisions by ablating the proposed architecture. We explore the effects of changing the number of layers, filter size, and the number of neighbors (K) for the dynamic stream. Finally, we control for the individual contribution of each stream.

We summarize our ablation results of the MAAS-TAN network in Table 2. In 2-a), we identify that the depth of the network is a relevant hyper-parameter for its performance. Shallow networks under-perform, but increasingly get better as we grow in depths, reaching an optimal value at 4 layers. Deeper networks have a better capacity for estimating useful features and have the chance to propagate relevant features over a large number of connected nodes, not only the immediate neighbors. In 2-b), we show that wider networks have a beneficial effect but saturate quickly with networks of 64 or more filters; beyond that size the networks do not yield improvements at the expense of additional network complexity. In 2-c), we demonstrate the complementary nature of the two stream proposal. While the static stream has the best individual performance, the dynamic stream is capable of finding relationships that are beyond the insights we use to create the static graph structure increasing the final performance by 0.9%. In section 4.4, we show some visualizations on the connections discovered by this stream to complement our analysis. Finally, 2-d) shows how the selected number of clusters on the dynamic stream affects the final performance of our method. Interestingly, the optimal numbers of neighbors is $K = 3$

Network Depth	mAP	Filters in Layer	mAP	Dynamic Graph	Static Graph	mAP	neighbors	mAP
1 Layer	88.0	32	88.5	✓	✗	66.5	2	88.5
2 Layer	88.2	64	88.8	✗	✓	87.9	3	88.8
3 Layer	88.4	128	88.6	✓	✓	88.8	4	88.4
4 Layer	88.8	256	88.1				5	88.4
5 Layer	87.5							

a) mAP by Network Depth **b)** mAP by Network Width **c)** mAP by Individual Stream **d)** mAP by clusters

Table 2. **Architecture choices** We ablate the design choices in the proposed graph neural network. We analyse the network depth in **a)**, and empirically find that deeper network favor the final result but saturates at 4 layer. We also analyse the number of filters per layer **b)** and find the optimal to be at 64. Regarding the dual stream **c)** we find the static stream to be far more effective, but the information extracted from the dynamic stream is still complementary. Finally **d)** we empirically find the more suitable number of neighbors and set it at 3.

which matches the number of valid assignments in the active speaker problem (audio with speech, active speaker), (audio with speech, silent speaker) and (audio with silence, silent speaker).

Graph Structure After assessing the design choices on the architecture, we proceed to evaluate the proposed graph structure. Here we test for the incremental addition of LAN graphs into a TAN graph that analyses N timestamps. Additionally we test for the maximum number of video nodes that get linked to an audio node at training time.

Number of LANs	Per LAN Video Nodes				
	1	2	3	4	5
1	80.2	84.3	84.9	85.1	85
5	85.4	87.1	87.3	87.4	87.3
9	86.6	87.8	87.9	88.3	88.5
13	87.1	88.1	88.4	88.8	88.5

Table 3. **Graph Structure.** We ablate the size of the MAAS-TAN network which is the core data structure of our approach. We empirically find it beneficial to model multiple speakers at the same time, and find the optimal number of speakers to be 4. Likewise, longer temporal sampling favors the performance but diminishes with sequences longer than 13 frames.

Overall, we notice that the MAAS network benefits from modelling longer temporal sequences or modelling more visible speakers. We interpret this as a consequence of our modelling strategy which is focused on the assignment of locally consistent visual and audio patterns, but remains compatible with the main stream approach of modelling long-term temporal sequences.

Supervision Finally, we assess the relevance of supervision for audio nodes, we empirically find that supervision over the video nodes provides most of the performance in MAAS. Nevertheless, supervising the audio nodes provides a small improvement on the final performance we think this extra supervision source allows for better estimation of the speech events, mitigating some false positives on the speaker detection.

Audio Supervision	Visual Supervision	mAP
✗	✓	88.5
✓	✓	88.8

Table 4. **Contribution of multi-modal Supervision.** We control the contribution of the individual supervision sources, we see that the network only loses 0.3% in performance if the audio supervision is lost. The direct audio supervision allows for slightly better estimation of speech events, thus refining the final active speaker assignment.

4.3. Dataset properties

Finally, we complement our analysis and follow the evaluation strategy of [40], we report the performance our method in known hard scenarios: small faces and multiple possible speakers.

We summarize the results for the face size in Table 5. Overall, we see a significant performance increase when comparing MAAS to the AVA baseline [40], and improvements in any scenario when compared to the multi-speaker stack of [2]. Clearly the multi-speaker scenario is still a challenging setup, but our improvements highlight that our proposal based on speech assignment is specially effective when we observe 2 or more possible speakers.

Number of Faces	MAAS	AVA Baseline [40]	ASC [2]
1	93.3	87.9	91.8
2	85.8	71.6	83.8
3	68.2	54.4	67.6

Table 5. **Performance evaluation by number of faces** We analyze the performance of our method according to the number of visible faces on the frame. While performance decreases the more people is visible, our method outperforms the AVA baseline and current state-of-the-art.

Table 6 contains the result for different sizes in the face crop. We follow the evaluation procedure of [40], and split the validation set into three mutually exclusive groups according to the observed size of the face. We create 3 sets: (S) with small sized faces that are smaller than 64x64 pixels, (M) with medium sized faces that are between 64x64 and 128x128 pixels and (L) with large faces that include

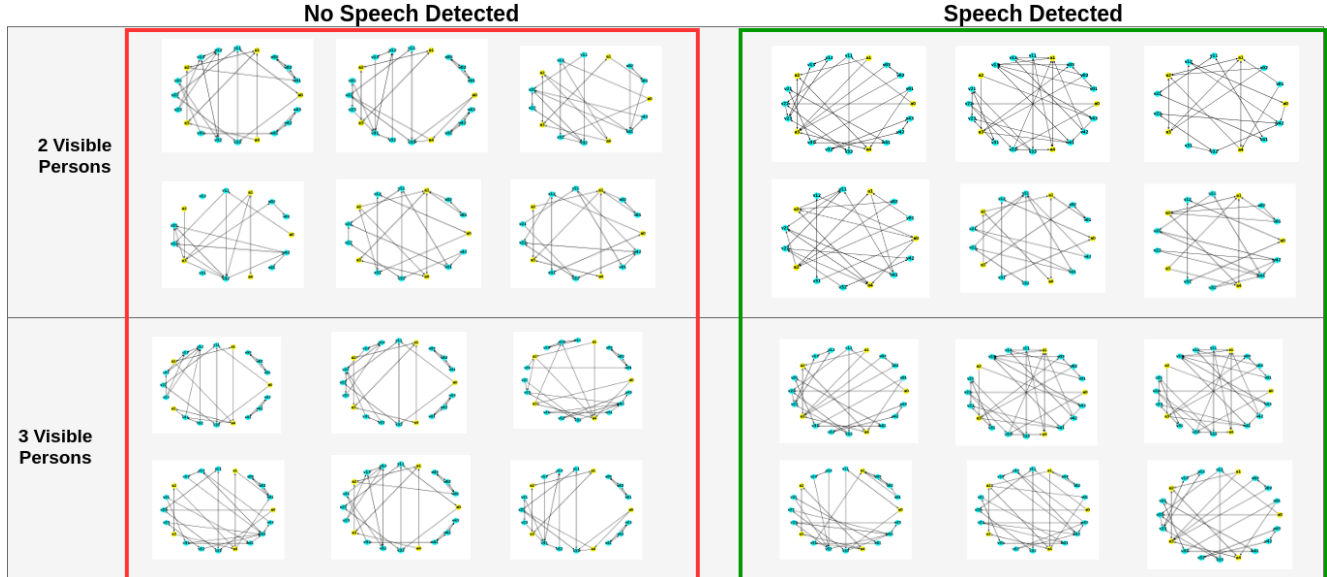


Figure 5. **Dynamic Graphs.** Our approach includes a dynamic stream, that creates graph structures from the nearest neighbours. The connections patterns in this stream are very diverse, but they follow some patterns according to the ground-truth of the nodes in the graph. For graphs with no speech events, we see connectivity is mostly between visual nodes on the same frame, and across frames on the audio nodes. For graphs that model speech events the connectivity is more diverse, and includes visual features across frames.

any face larger than 128x128 pixels. Our approach does not directly addresses the image size, nevertheless, we notice a large performance gap when compared to the AVA baseline, and we improve in most scenarios when compared to the method of Alcazar *et al.* We believe this increase in performance is related to better predictions in related faces, that is, smaller faces are typically seen in cluttered scenes with multiple other visible persons, our method improves the prediction on these smaller faces by integrating more reliable information from other speakers.

Face Size	MAAS	AVA Baseline [40]	ASC [2]
S	55.2	44.9	56.2
M	79.4	68.3	79.0
L	93.0	86.4	92.2

Table 6. **Performance evaluation by number of faces** We asses the performance of our method in another challenging scenario, small and medium size faces, we define small faces as those that cover less than 64x64 pixels, and medium as less than 128x128 pixels. We observe that our methods outperform the current state-of-the-art, in every scenario, except for the smaller faces.

4.4. Qualitative Analysis

We conclude our analysis by briefly looking at the graphs structures estimated by the dynamic stream. As we see in Figure 5 the graph structure is highly variable. Nevertheless we do find a significant pattern when we group the graphs according to the ground-truth of the segment.

We observe that graphs that do not contain speech events (left in the red box) usually have more bidirectional con-

nections between the visual nodes of a single frame, and a few connections between the audio nodes, or across frames. This structure resembles the local assignation graphs, and our interpretation is that silent segments contain very little ambiguity so additional connections bring little improvement on the predictions.

The graphs where speech events are detected, have a lot more unidirectional connections between audio and visual nodes that belong too different frames, as consequence they look as if the had more connections in Figure 5, our hypothesis is that, in the presence of speech, the dynamic stream tries to generate multiple new connections, aggregating global information into a few nodes that seem to be more relevant in the assignation process.

5. Conclusion

I this work, we have introduced MAAS a novel multi-modal assignation technique based on graph convolutional networks, devised for the active speaker detection task. Our method departs from the standard procedure of estimating audiovisual embeddings that are suitable for binary predictions, and focuses on optimizing a graph neural network that estimates the best source (active speaker) for an speech event. MAAS-TAN achieves state-of-the-art performance in the large scale AVA-active speaker dataset, as a direct consequence of its novel assignation mechanism, also improving performance over state-of-the-art techniques in well known failure scenarios.

References

- [1] Triantafyllos Afouras, Andrew Owens, Joon Son Chung, and Andrew Zisserman. Self-supervised learning of audio-visual objects from video. *arXiv preprint arXiv:2008.04237*, 2020.
- [2] Juan Leon Alcazar, Fabian Caba, Long Mai, Federico Perazzi, Joon-Young Lee, Pablo Arbelaez, and Bernard Ghanem. Active speakers in context. In *Proceedings of the IEEE/CVF Conference on Computer Vision and Pattern Recognition*, pages 12465–12474, 2020.
- [3] Xavier Anguera, Simon Bozonnet, Nicholas Evans, Corinne Fredouille, Gerald Friedland, and Oriol Vinyals. Speaker diarization: A review of recent research. *IEEE Transactions on Audio, Speech, and Language Processing*, 20(2):356–370, 2012.
- [4] Punarjay Chakravarty, Sayeh Mirzaei, Tinne Tuytelaars, and Hugo Van hamme. Who’s speaking? audio-supervised classification of active speakers in video. In *International Conference on Multimodal Interaction (ICMI)*, 2015.
- [5] Punarjay Chakravarty, Jeroen Zegers, Tinne Tuytelaars, et al. Active speaker detection with audio-visual co-training. In *International Conference on Multimodal Interaction (ICMI)*, 2016.
- [6] Joon Son Chung. Naver at activitynet challenge 2019–task b active speaker detection (ava). *arXiv preprint arXiv:1906.10555*, 2019.
- [7] Joon Son Chung, Arsha Nagrani, and Andrew Zisserman. Voxceleb2: Deep speaker recognition. *arXiv preprint arXiv:1806.05622*, 2018.
- [8] Joon Son Chung, Andrew Senior, Oriol Vinyals, and Andrew Zisserman. Lip reading sentences in the wild. In *CVPR*, 2017.
- [9] Joon Son Chung and Andrew Zisserman. Out of time: automated lip sync in the wild. In *ACCV*, 2016.
- [10] Soo-Whan Chung, Joon Son Chung, and Hong-Goo Kang. Perfect match: Improved cross-modal embeddings for audio-visual synchronisation. In *IEEE International Conference on Acoustics, Speech and Signal Processing (ICASSP)*, 2019.
- [11] Ross Cutler and Larry Davis. Look who’s talking: Speaker detection using video and audio correlation. In *International Conference on Multimedia and Expo*, 2000.
- [12] Jia Deng, Wei Dong, Richard Socher, Li-Jia Li, Kai Li, and Li Fei-Fei. Imagenet: A large-scale hierarchical image database. In *CVPR*, 2009.
- [13] Mark Everingham, Josef Sivic, and Andrew Zisserman. Taking the bite out of automated naming of characters in tv video. *Image and Vision Computing*, 27(5):545–559, 2009.
- [14] Matthias Fey and Jan E. Lenssen. Fast graph representation learning with PyTorch Geometric. In *ICLR Workshop on Representation Learning on Graphs and Manifolds*, 2019.
- [15] Daniel Garcia-Romero, David Snyder, Gregory Sell, Daniel Povey, and Alan McCree. Speaker diarization using deep neural network embeddings. In *2017 IEEE International Conference on Acoustics, Speech and Signal Processing (ICASSP)*, pages 4930–4934. IEEE, 2017.
- [16] Georgia Gkioxari, Jitendra Malik, and Justin Johnson. Mesh r-cnn. *arXiv preprint arXiv:1906.02739*, 2019.
- [17] Raia Hadsell, Sumit Chopra, and Yann LeCun. Dimensionality reduction by learning an invariant mapping. In *CVPR*, 2006.
- [18] Kaiming He, Xiangyu Zhang, Shaoqing Ren, and Jian Sun. Deep residual learning for image recognition. In *CVPR*, 2016.
- [19] Kaiming He, Xiangyu Zhang, Shaoqing Ren, and Jian Sun. Identity mappings in deep residual networks. In *European conference on computer vision*, pages 630–645. Springer, 2016.
- [20] Ashesh Jain, Amir R Zamir, Silvio Savarese, and Ashutosh Saxena. Structural-rnn: Deep learning on spatio-temporal graphs. In *Proceedings of the IEEE Conference on Computer Vision and Pattern Recognition*, pages 5308–5317, 2016.
- [21] Arindam Jati and Panayiotis Georgiou. Neural predictive coding using convolutional neural networks toward unsupervised learning of speaker characteristics. *IEEE/ACM Transactions on Audio, Speech, and Language Processing*, 27(10):1577–1589, 2019.
- [22] Justin Johnson, Agrim Gupta, and Li Fei-Fei. Image generation from scene graphs. In *Proceedings of the IEEE Conference on Computer Vision and Pattern Recognition*, pages 1219–1228, 2018.
- [23] Andrej Karpathy, George Toderici, Sanketh Shetty, Thomas Leung, Rahul Sukthankar, and Li Fei-Fei. Large-scale video classification with convolutional neural networks. In *Proceedings of the IEEE conference on Computer Vision and Pattern Recognition*, pages 1725–1732, 2014.
- [24] Changil Kim, Hujung Valentina Shin, Tae-Hyun Oh, Alexandre Kaspar, Mohamed Elgharib, and Wojciech Matusik. On learning associations of faces and voices. In *ACCV*, 2018.
- [25] D Kinga and J Ba Adam. A method for stochastic optimization. In *ICLR*, 2015.
- [26] Thomas N Kipf and Max Welling. Semi-supervised classification with graph convolutional networks. *arXiv preprint arXiv:1609.02907*, 2016.
- [27] Guohao Li, Matthias Muller, Ali Thabet, and Bernard Ghanem. Deepgcns: Can gcns go as deep as cnns? In *The IEEE International Conference on Computer Vision (ICCV)*, 2019.
- [28] Guohao Li, Matthias Müller, Guocheng Qian, Itzel C. Delgadillo, Abdullellah Abualshour, Ali Thabet, and Bernard Ghanem. Deepgcns: Making gcns go as deep as cnns, 2019.
- [29] Guohao Li, Guocheng Qian, Itzel C. Delgadillo, Matthias Müller, Ali Thabet, and Bernard Ghanem. Sgas: Sequential greedy architecture search, 2019.
- [30] Guohao Li, Chenxin Xiong, Ali Thabet, and Bernard Ghanem. Deeppergcn: All you need to train deeper gcns. *arXiv preprint arXiv:2006.07739*, 2020.
- [31] Yikang Li, Wanli Ouyang, Bolei Zhou, Jianping Shi, Chao Zhang, and Xiaogang Wang. Factorizable net: an efficient subgraph-based framework for scene graph generation. In *Proceedings of the European Conference on Computer Vision (ECCV)*, pages 335–351, 2018.
- [32] Arsha Nagrani, Samuel Albanie, and Andrew Zisserman. Learnable pins: Cross-modal embeddings for person identity. In *ECCV*, 2018.

- [33] Arsha Nagrani, Samuel Albanie, and Andrew Zisserman. Seeing voices and hearing faces: Cross-modal biometric matching. In *CVPR*, 2018.
- [34] Arsha Nagrani, Joon Son Chung, and Andrew Zisserman. Voxceleb: a large-scale speaker identification dataset. *arXiv preprint arXiv:1706.08612*, 2017.
- [35] Jiquan Ngiam, Aditya Khosla, Mingyu Kim, Juhan Nam, Honglak Lee, and Andrew Y Ng. Multimodal deep learning. In *ICML*, 2011.
- [36] Andrew Owens and Alexei A Efros. Audio-visual scene analysis with self-supervised multisensory features. In *Proceedings of the European Conference on Computer Vision (ECCV)*, pages 631–648, 2018.
- [37] Adam Paszke, Sam Gross, Soumith Chintala, Gregory Chanan, Edward Yang, Zachary DeVito, Zeming Lin, Alban Desmaison, Luca Antiga, and Adam Lerer. Automatic differentiation in pytorch. In *NeurIPS-Workshop*, 2017.
- [38] Xiaojuan Qi, Renjie Liao, Jiaya Jia, Sanja Fidler, and Raquel Urtasun. 3d graph neural networks for rgbd semantic segmentation. In *Proceedings of the IEEE International Conference on Computer Vision*, pages 5199–5208, 2017.
- [39] Mirco Ravanelli and Yoshua Bengio. Speaker recognition from raw waveform with sincnet. In *IEEE Spoken Language Technology Workshop (SLT)*, 2018.
- [40] Joseph Roth, Sourish Chaudhuri, Ondrej Klejch, Radhika Marvin, Andrew Gallagher, Liat Kaver, Sharadh Ramaswamy, Arkadiusz Stopczynski, Cordelia Schmid, Zhonghua Xi, et al. Ava-activespeaker: An audio-visual dataset for active speaker detection. *arXiv preprint arXiv:1901.01342*, 2019.
- [41] Kate Saenko, Karen Livescu, Michael Siracusa, Kevin Wilson, James Glass, and Trevor Darrell. Visual speech recognition with loosely synchronized feature streams. In *ICCV*, 2005.
- [42] Rahul Sharma, Krishna Somandepalli, and Shrikanth Narayanan. Crossmodal learning for audio-visual speech event localization. *arXiv preprint arXiv:2003.04358*, 2020.
- [43] Stephen H Shum, Najim Dehak, Réda Dehak, and James R Glass. Unsupervised methods for speaker diarization: An integrated and iterative approach. *IEEE Transactions on Audio, Speech, and Language Processing*, 21(10):2015–2028, 2013.
- [44] Fei Tao and Carlos Busso. Bimodal recurrent neural network for audiovisual voice activity detection. In *INTERSPEECH*, pages 1938–1942, 2017.
- [45] Sue E Tranter and Douglas A Reynolds. An overview of automatic speaker diarization systems. *IEEE Transactions on audio, speech, and language processing*, 14(5):1557–1565, 2006.
- [46] Alex Waibel, Toshiyuki Hanazawa, Geoffrey Hinton, Kiyohiro Shikano, and Kevin J Lang. Phoneme recognition using time-delay neural networks. *IEEE transactions on acoustics, speech, and signal processing*, 37(3):328–339, 1989.
- [47] Quan Wang, Carlton Downey, Li Wan, Philip Andrew Mansfield, and Ignacio Lopez Moreno. Speaker diarization with lstm. In *2018 IEEE International Conference on Acoustics, Speech and Signal Processing (ICASSP)*, pages 5239–5243. IEEE, 2018.
- [48] Quan Wang, Hannah Muckenhirn, Kevin Wilson, Prashant Sridhar, Zelin Wu, John Hershey, Rif A Saurous, Ron J Weiss, Ye Jia, and Ignacio Lopez Moreno. Voicefilter: Targeted voice separation by speaker-conditioned spectrogram masking. *arXiv preprint arXiv:1810.04826*, 2018.
- [49] Yue Wang, Yongbin Sun, Ziwei Liu, Sanjay Sarma, Michael Bronstein, and Justin Solomon. Dynamic graph cnn for learning on point clouds. *ACM Transactions on Graphics*, 2018.
- [50] Yue Wang, Yongbin Sun, Ziwei Liu, Sanjay E Sarma, Michael M Bronstein, and Justin M Solomon. Dynamic graph cnn for learning on point clouds. *Acm Transactions On Graphics (tog)*, 38(5):1–12, 2019.
- [51] Zhuyang Xie, Junzhou Chen, and Bo Peng. Point clouds learning with attention-based graph convolution networks. *arXiv preprint arXiv:1905.13445*, 2019.
- [52] Danfei Xu, Yuke Zhu, Christopher B Choy, and Li Fei-Fei. Scene graph generation by iterative message passing. In *Proceedings of the IEEE Conference on Computer Vision and Pattern Recognition*, pages 5410–5419, 2017.
- [53] Mengmeng Xu, Chen Zhao, David S Rojas, Ali Thabet, and Bernard Ghanem. G-tad: Sub-graph localization for temporal action detection. In *Proceedings of the IEEE/CVF Conference on Computer Vision and Pattern Recognition*, pages 10156–10165, 2020.
- [54] Sarthak Yadav and Atul Rai. Learning discriminative features for speaker identification and verification. In *Inter-speech*, 2018.
- [55] Sijie Yan, Yuanjun Xiong, and Dahua Lin. Spatial temporal graph convolutional networks for skeleton-based action recognition. In *Thirty-Second AAAI Conference on Artificial Intelligence*, 2018.
- [56] Jianwei Yang, Jiasen Lu, Stefan Lee, Dhruv Batra, and Devi Parikh. Graph r-cnn for scene graph generation. In *Proceedings of the European Conference on Computer Vision (ECCV)*, pages 670–685, 2018.
- [57] Chengzhu Yu and John HL Hansen. Active learning based constrained clustering for speaker diarization. *IEEE/ACM Transactions on Audio, Speech, and Language Processing*, 25(11):2188–2198, 2017.
- [58] Aonan Zhang, Quan Wang, Zhenyao Zhu, John Paisley, and Chong Wang. Fully supervised speaker diarization. In *IEEE International Conference on Acoustics, Speech and Signal Processing (ICASSP)*. IEEE, 2019.
- [59] Yuan-Hang Zhang, Jingyun Xiao, Shuang Yang, and Shiguang Shan. Multi-task learning for audio-visual active speaker detection.